Journal of Crystal Growth 378 (2013) 537–541

Contents lists available at SciVerse ScienceDirect

Journal of Crystal Growth

journal homepage: www.elsevier.com/locate/jcrysgro

Infrared emitting property and spherical symmetry of colloidal PbS quantum dots

Seisuke Nakashima [a,b,*], Kosuke Kikushima [a], Kohki Mukai [a]

[a] Department of Solid State Materials and Engineering, Yokohama National University, 79-5 Tokiwadai, Hodogaya-ku, Yokohama-shi, Kanagawa 240-8501, Japan

[b] RIKEN—Advanced Research Institute, 2-1 Hirosawa, Wako-shi, Saitama 351-0198, Japan

ARTICLE INFO

Available online 29 January 2013

Keywords:
A1. Nanostructures
A1. Quantum dots
B1. Nanomaterials
B1. Sulfides
B2. Semiconducting lead compounds
B3. Infrared devices

ABSTRACT

Infrared emitting properties and spherical symmetry of colloidal PbS quantum dots (QDs) chemically synthesized in organic solvent oleylamin as a ligand were investigated in terms of synthesis temperature, time, and precursor concentrations. The progress of the nucleation process and crystal growth of PbS nanocrystals can be interpreted using the LaMer mechanism. By decreasing the temperature or increasing the concentration of precursors, the degree of supersaturation becomes higher, resulting in precipitation of small nuclei. Meanwhile, in the case of the lower supersaturation, the particle size and the size distribution of nanocrystals become larger and narrower. Direct evaluations of the spherical symmetry of the synthesized QDs were carried out using symmetry indexes derived from the transmission electron microscopy images. These results clearly indicated that lower reaction temperature, higher supersaturation, and longer growing time are favorable for the synthesis of spherical QDs emitting at the wavelength of the 1.3 μm region.

1. Introduction

The semiconductor quantum dot (QD) is actively studied for advanced applications in a variety of fields, such as biomedical engineering, solar cells, optical communication, [1–6] due to the wide-range spectral tunability. For the purpose of developing quantum communication and quantum information technologies, in particular, perfectly symmetrical (spherical) QDs emitting in the infrared range are required as a source of entangled photon pairs. However, the epitaxial QDs grown on substrates possess shape anisotropy, which is caused by the lattice mismatch and the anisotropy in the atomic arrangement of crystalline surface [7]. In contrast, colloidal synthesis methods in liquid solvent are free from the substrate restriction, and therefore, the highly spherical QDs are expected to be created easily compared with the epitaxial growth methods.

The spherical symmetry of colloidal QDs is strongly influenced by several synthesis conditions, such as precursor concentrations, synthesis temperature, and so on. Hence, further detailed understanding of the mechanism of crystal growth is quite important for the control of shape symmetry of QDs. It is well known that the synthesis of QDs in organic solvent conforms to the LaMer mechanism [8]. The LaMer diagram schematically illustrates how the rapid nucleation and the subsequent crystal growth progress under the continuous supply of monomers. In the initial nucleation stage, the critical nuclear radius and the shape symmetry are determined by the degree of supersaturation, which depends on the temperature and the concentration of precursors. In the subsequent growth stage, the nucleation stops, since the concentration of precursors falls below the critical supersaturation. Then, the size and the spherical symmetry of QDs will be gradually changed until the precursor concentrations settle down to the saturation solubility.

From the viewpoint of application for information–communication technology in the NIR spectral region, lead sulfide (PbS) nanocrystals is one of the most promising materials. Hines and Scholes for the first time reported the organometallic synthesis of PbS QDs with size-tunable emission in the NIR region using oleic acid as a ligand, and lead oxide and bis(trimethilsilyl) sulfide ($(TMS)_2S$) as precursors [9]. Ozin's group successfully synthesized PbS QDs with narrow size distribution by applying the hot injection method to the viscous reaction system due to high concentration of $PbCl_2$ [10]. Recently, the ligand and precursor effects on the crystal growth and optical properties of PbS QDs have been systematically studied [11,12]. In this paper, the correlation between the emission properties and the spherical symmetry of PbS QDs has been investigated in terms of synthesis

* Corresponding author at: Department of Solid State Materials and Engineering, Yokohama National University, 79-5 Tokiwadai, Hodogaya-Ku, Yokohama-shi, Kanagawa 240-8501, Japan.
E-mail address: nakashima@ynu.ac.jp (S. Nakashima).

0022-0248/$ - see front matter © 2013 Elsevier B.V. All rights reserved.
http://dx.doi.org/10.1016/j.jcrysgro.2012.12.132

temperature, time, and precursor concentrations. We have also explored synthetic conditions suited for the emission at the wavelength of the 1.3 μm region, which is potentially advantageous for the utilization of the existing fiber communication systems. Then, the spherical symmetry of synthesized QDs was directly evaluated using symmetry indexes which were statistically calculated using transmission electron microscopy (TEM) images. At present, the control of the spherical symmetry for colloidal nanocrystals is a difficult and challenging trial although a variety of shapes of PbS micro- or submicro-crystals have been already examined [13,14].

2. Experimental

PbS QDs were synthesized by the hot injection method [15] using oleylamine (OLA) as the ligand. $PbCl_2$ (0.56 g) and 10 ml of OLA were loaded into a three-neck flask at room temperature. The mixture was magnetically stirred and heated to the synthesis temperature to form the homogeneous $PbCl_2$–OLA suspension while the flask was purged by N_2. The synthesis temperature was set at 70 and 80 °C. At the same time, 0.16 g of sulfur was dissolved in 15 ml of OLA and the solution was kept at 120 °C for 30 min. The sulfur–OLA solution was then quickly injected into the flask under vigorous stirring, and the reaction was allowed to continue at the same temperature for 1–25 min to obtain PbS QDs of different sizes. For each synthesis time, aliquots of the solution were taken from the flask and quenched by cold hexane. The solution with the addition of methanol was centrifuged to remove excess OLA. Then, the precipitate was redispersed in hexane. Photoluminescence (PL) spectra for the solution dispersed with PbS QDs were measured at room temperature by using a 635 nm laser diode as a pump. The particle size and shape symmetry were directly examined by TEM measurement using a JEOL JEM2100F at 200 kV.

3. Results and discussions

In a LaMer diagram [9], the particle formation process consists of two stages: a nucleation stage (Stage I), and a growth stage (Stage II). In the first stage where the solution concentration reaches the critical supersaturation, the nucleation process starts. The nuclear size is determined by the synthesis temperature and the degree of supersaturation. The critical radius of nuclei is given by

$$r_c = 2\gamma v/RT\ln\sigma \quad (1)$$

where γ is the interface energy, v is the molar volume of the crystalline phase, R is the gas constant, T is the absolute temperature, and σ is the degree of supersaturation. The equation represents that the critical nuclear radius is inversely proportional to a logarithm of the degree of supersaturation, which depends on the saturating concentration and the concentrations of precursors. After nucleation, the solution concentration begins to decrease and falls below the critical supersaturation again, then the growth stage starts. In Stage II, the nuclei grow and the QD size increases. Then the solution concentration settles down to the saturation solubility and the growth of QDs almost completely stops.

Fig. 1 shows the evolution of PL spectra with respect to time during the growth of the PbS QDs synthesized at (a) 70 and (b) 80 °C, when the molar ratio of precursors, $PbCl_2$:S:OLA = 10:1:24. The full width at half maximum (FWHM) and the wavelength of the luminescence peak are also plotted as a function of synthesis time in Fig. 1(c) and (d). With the synthesis time increasing from 1 to

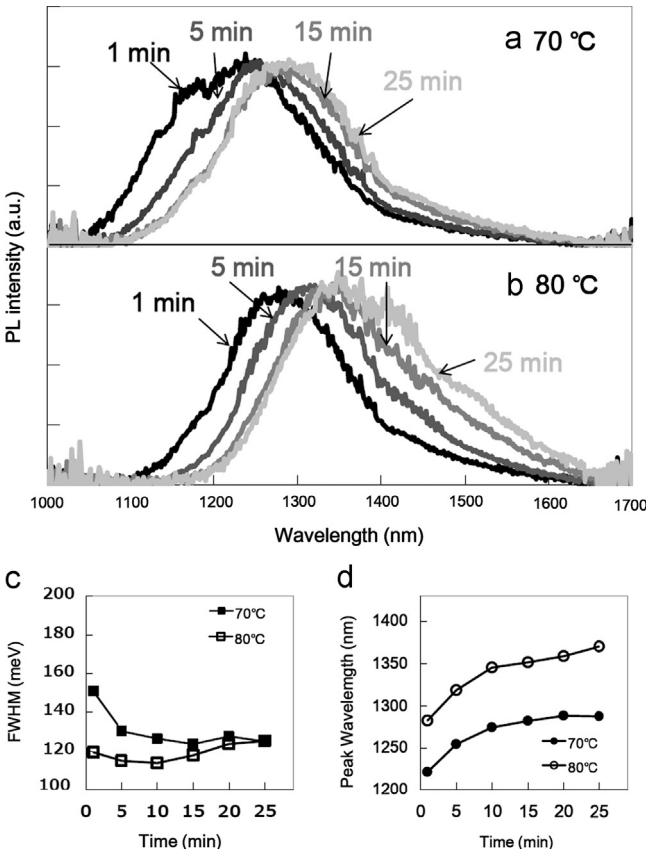

Fig. 1. Time evolution of PL spectra of the PbS QDs synthesized at (a) 70 and (b) 80 °C, when the molar ratio of precursors is $PbCl_2$:S:OLA = 10:1:24. (c) Full width at half maximum (FWHM) and (d) the peak wavelength of the luminescence peak plotted as a function of synthesis time.

25 min, the luminescence wavelength of the QDs exhibits red shifts of 1221–1288 nm for 70 °C and of 1282–1370 nm for 80 °C. These peak shifts correspond to the increases in the size of QDs. In both cases, the nucleation of PbS nanocrystals in the initial stage immediately finishes, and then the crystal growth starts and the growth rate gradually slows down. This means that the growth rate depends on the amount of available precursors. A notable difference in the wavelength after 1 min between these two temperatures can be observed, which suggests that the critical radius, r_c, of the PbS nuclei synthesized at 80 °C is larger than that of the nuclei synthesized at 70 °C. Generally, the saturating solubility of precursors increases at higher temperatures. Therefore, in the synthesis condition at 80 °C, the supersaturation, σ, is lower than that for 70 °C. According to Eq. (1), the lower σ at 80 °C gives rise to a larger r_c compared with the case of 70 °C, even though T becomes higher. In this case, the critical supersaturation also increases, which makes the duration time of the nucleation stage shorter. As a result, the size distribution of PbS nuclei becomes narrower, which is consistent with the fact that the FWHM of the luminescence peak for 80 °C is totally smaller than for 70 °C. After 10 min, however, the FWHM of the luminescence peak for 70 °C rapidly decreased, while that for 80 °C slightly but clearly increases. This increase is presumably due to the effects of Ostwald ripening or agglomeration.

Fig. 2 displays the bright-field TEM images of PbS QDs synthesized for 1 and 15 min at 70 and 80 °C, respectively. The insets show the size frequency histograms for the QDs. The estimated values of the QD sizes and the standard deviations were summarized in Table 1. With increase in the temperature and the synthesis time, the average size increases and the standard deviation decreases. The tendencies are mostly

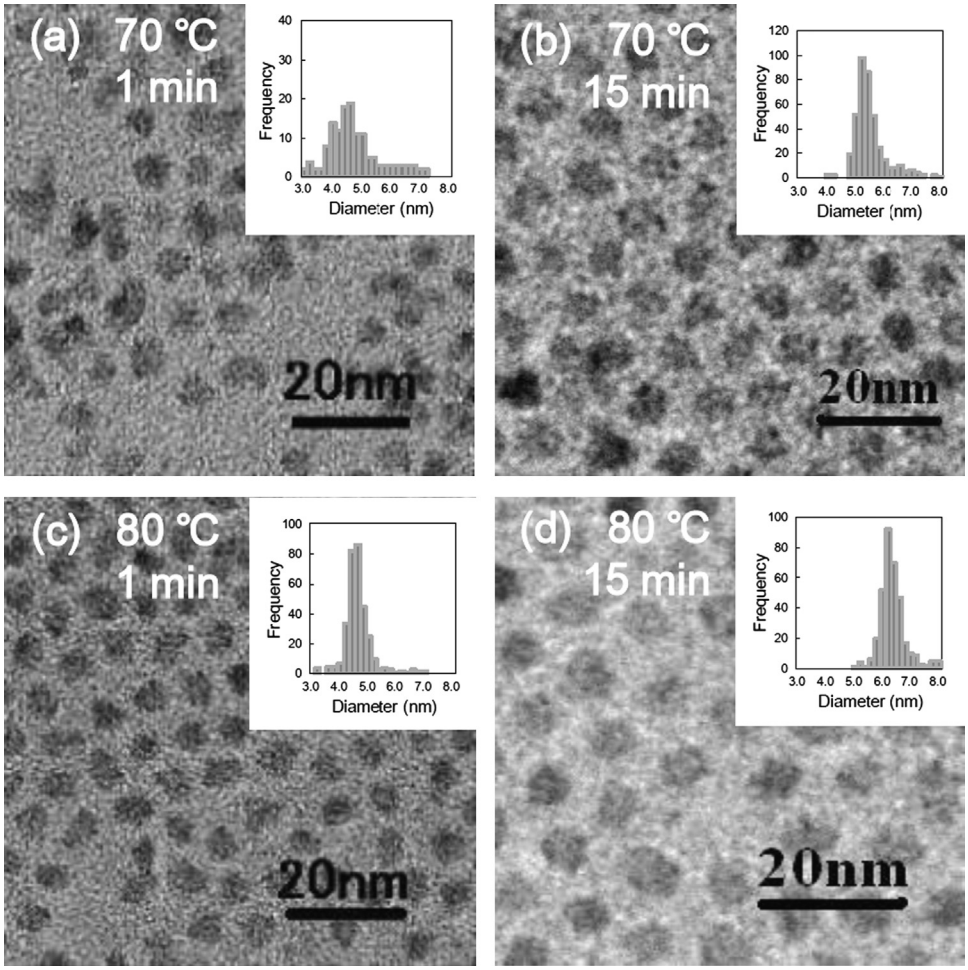

Fig. 2. Bright-field TEM images of PbS QDs synthesized at 70 °C for (a) 1 min and (b) 15 min and at 80 °C for (c) 1 min and (d) 15 min. Insets: histograms of QD size.

Table 1
QD average sizes, standard deviations, and symmetry indexes analyzed using the TEM images.

Temperature (°C)	70		80	
Synthesis time (min)	1	15	1	15
Average size (nm)	4.47	5.30	4.53	6.27
Standard deviation	0.920	0.572	0.527	0.468
Symmetry index	0.60	0.72	0.58	0.63

consistent with the increase in the wavelength of PL emission peak and the decrease in the FWHM, as shown in Fig. 1.

We also changed the amount and the ratio of precursors to investigate the effect of these conditions on the crystal growth and the size uniformity of QDs. The time evolution of PL spectra for PbS QDs synthesized at 70 °C at the $PbCl_2$:S:OLA ratio of 7.5:0.75:24 is shown in Fig. 3(a). The FWHM and the wavelength of the PL peak are plotted in Fig. 3(b) and (c), respectively. Compared with the QDs synthesized at the $PbCl_2$:S:OLA ratio of 10:1:24, a wider wavelength shift from 1239 to 1327 nm and relatively narrower FWHMs were observed. In the lower concentration of precursors, the degree of the supersaturation, σ, was decreased, resulting in a short nucleation stage. The number of PbS nuclei that grew within the short period of time is so small that the size distribution would become narrower. In addition, the low σ provides a situation in which larger-critical-radius nuclei are energetically stable (Eq. (1)). Therefore, the crystal growth of

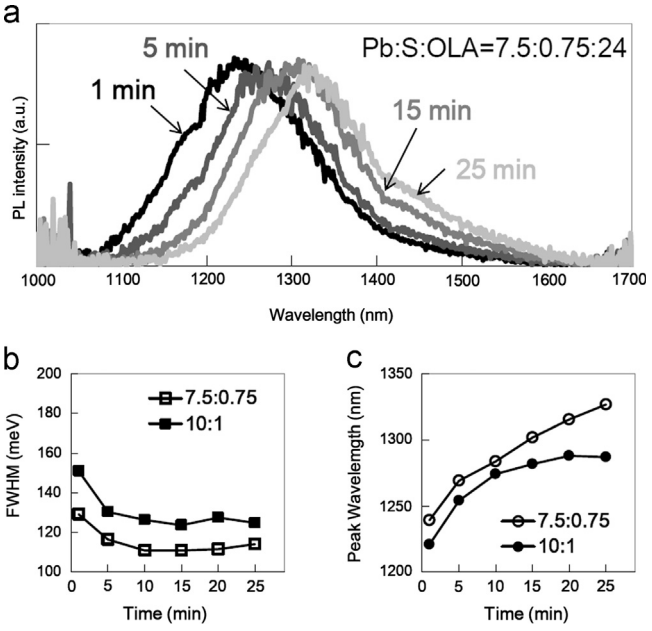

Fig. 3. (a) Time evolution of PL spectra of the PbS QDs synthesized at 70 °C when the molar ratio of precursors is $PbCl_2$:S:OLA=7.5:0.75:24. (b) Full width at half maximum (FWHM) and (c) the peak wavelength of the luminescence peak plotted as a function of synthesis time.

the nuclei progresses further into a size larger than that in the case of the higher σ.

In Fig. 4(a), the time evolution of PL spectra for PbS QDs synthesized at 80 °C at the $PbCl_2$:S:OLA ratio of 10:2:24 is shown. The variations of FWHM and the position of luminescence peaks as a function of synthesis time are also plotted in Fig. 4(b) and (c), respectively. The amount of available sulfur was doubled in this condition compared with the ratio of 10:1:24 (Fig. 1(b)). Hence, the supersaturation was relatively increased, leading to a longer time of nucleation stage. As a result, a wider size distribution of nuclei was obtained, as shown in Fig. 4(b). Meanwhile, the critical radius of QDs was expected to be smaller for a higher supersaturation condition. In Fig. 4(c), however, the luminescence peaks appeared at the longer wavelength compared to the ratio of 10:1:24, suggesting that larger particles were formed. This can be explained as follows. However, the critical radius at the $PbCl_2$:S:OLA ratio of 10:2:24 is relatively smaller in the nucleation stage. On the other hand, the doubled amount of sulfur presumably induces the significant increase in the number of PbS clusters. Unstable clusters, the size of which does not reach the critical radius, can contribute to the crystal growth, resulting in much higher growth rate. Therefore, after the nucleation stage, the size of PbS QDs rapidly increases, and then exceeds to that in the case of the ratio of 10:1:24. Zhao et al. also reported the peak shift as a function of synthesis time in a variety of ratios of precursors, which shows the same tendency as our results [11].

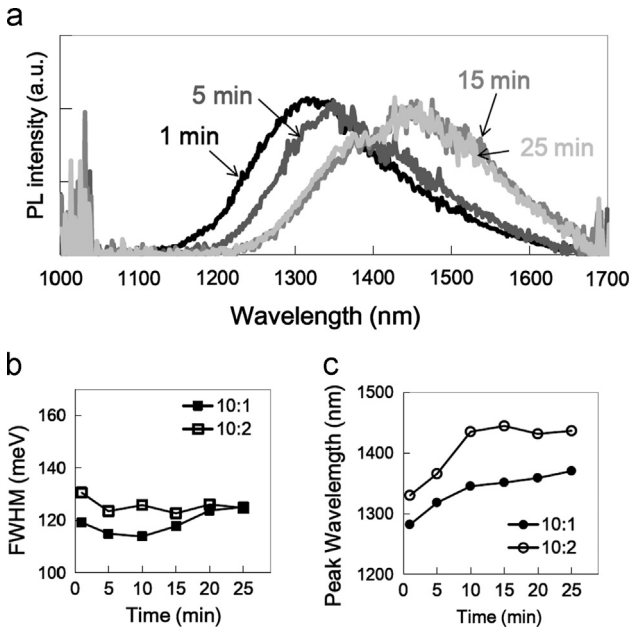

Fig. 4. (a) Time evolution of PL spectra of the PbS QDs synthesized at 80 °C when the molar ratio of precursors is $PbCl_2$:S:OLA=10:2:24. (b) Full width at half maximum (FWHM) and (c) the peak wavelength of the luminescence peak plotted as a function of synthesis time.

For the purpose of evaluating the suitability of the synthesized PbS NCs for the source of entangled photon pairs, quantitative measurement of spherical symmetry is particularly indispensable. Generally, the in-plane symmetry of the SK-type QDs can be examined using grazing-incidence X-ray diffraction (XRD). Since such QDs are epitaxially grown on single-crystal substrates, long axes of elongated NCs align along the specific crystalline orientation of substrates. By contrast, the shape of chemically synthesized colloidal NCs is not necessarily elongated or uniaxially anisotropic. In addition, since the NCs are dispersed with no orientation in aqueous solutions or organic solvents, the particles do not align along one direction. Thus, the measurements give spatially- and time-averaged information about the shape symmetry of NCs using grazing-incidence XRD. Therefore, direct evaluation of the spherical symmetry of QDs using the TEM results is the only available method at present. We selected about 200 particles at random in TEM images, and maximum inscribed circles and minimum circumscribed ones were systematically determined for each particle. A symmetry index is calculated as an average of the ratio of diameters (D_{min}/D_{max})

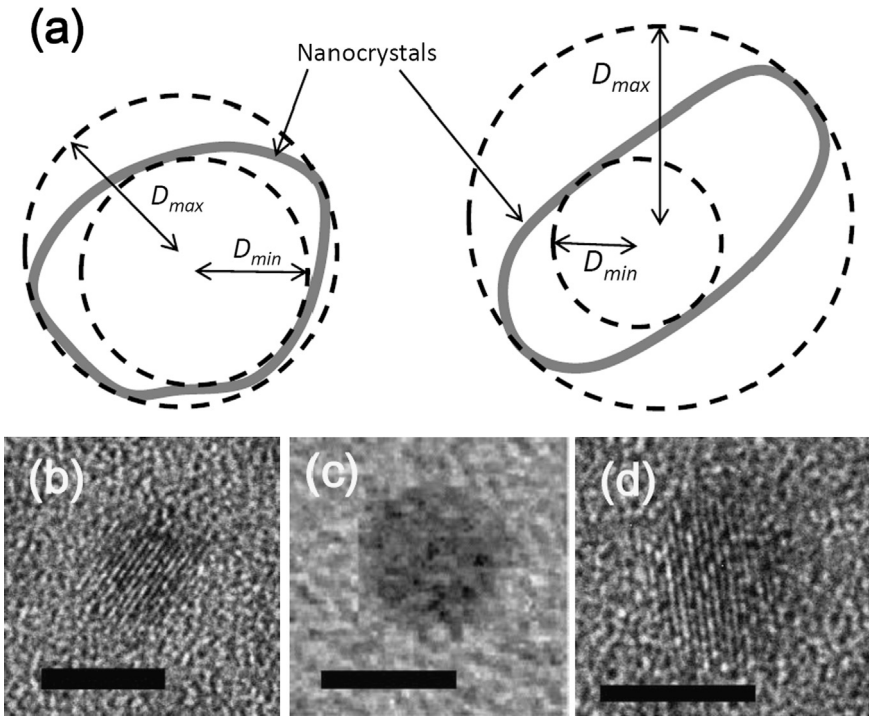

Fig. 5. (a) Schematic illustrations of the determination of symmetry indexes for distorted nanocrystals. High resolution TEM images of QDs synthesized (b) at 70 °C for 15 min at $PbCl_2$:S:OLA=10:1:24 (c) at 80 °C for 1 min at $PbCl_2$:S:OLA=10:1:24, and (d) at 80 °C for 5 min at $PbCl_2$:S:OLA=2:1:24. The scale bars represent 5 nm.

for all of the particles, as illustrated in Fig. 5(a). High-resolution TEM images of these PbS QDs synthesized at three different conditions are shown in Fig. 5(b)–(d). The calculated index values are summarized in Table 1 for the PbS QDs synthesized for 1 and 15 min at 70 and 80 °C, respectively. For lower synthesis temperature and longer synthesis time, the symmetry index tended to be higher. Since higher temperature is advantageous for the homogeneity of the particle size, it is difficult to obtain QDs with both highly spherical symmetry and narrow size distribution. According to Fig. 1(d), the PbS QDs synthesized under the two different conditions (at 70 °C for 15 min and at 80 °C for 1 min) provided the luminescence peaks at the same wavelength of 1282 nm. The estimated symmetry indexes were 0.72 for the former and 0.58 for the latter. For the lower synthesis temperature, that is, the higher supersaturation, a relatively larger number of small nuclei will be precipitated at the first nucleation stage, leading to the slower-rate growth of the particle, which is consistent with the fact that the PL-peak shift at the condition of 70 °C is smaller than that of 80 °C. If the particle growth progressed rapidly, the spherical symmetry of QDs would be expected to be lower because of an anisotropic crystal growth in directions preferable for a stable crystal structure. Thus, it is speculated that the highly symmetrical PbS QDs were achieved due to the slower-rate condition induced by the higher supersaturation.

4. Conclusions

Colloidal PbS QDs were chemically synthesized in organic solvent, OLA, as a ligand under a variety of conditions. At lower synthetic temperature or higher concentration of precursors, the degree of supersaturation becomes higher, leading to the precipitation of larger amount of nuclei with a smaller critical radius. In this case, the PL peaks had a relatively wide FWHM, suggesting the wide distribution of particle size of the nuclei. In contrast, at higher temperature or lower precursor concentrations giving rise to lower supersaturation, the larger particle size and the narrower distribution of PbS nanocrystals can be obtained. Symmetry indexes for PbS QDs with diameters of about 1.3 μm were evaluated using TEM images. This comparison clarified that lower reaction temperature, higher supersaturation, and longer growing time are suited for the synthesis of spherical PbS QDs which can be a promising candidate as the source of entangled photon pairs in the infrared region.

Acknowledgments

This study was financially supported by Grants-in-Aids for Scientific Research (B) and Young Scientists (B) from the Ministry of Education, Culture, Sports, Science, and Technology (MEXT), Japan, and by the Nippon Sheet Glass Foundation for Materials Science and Engineering.

References

[1] M. Bruchez, M. Moronne, P. Gin, S. Weiss, A.P. Alivisatos, Science 281 (1998) 2013.
[2] W.C.W. Chan, S. Nie, Science 281 (1998) 2016.
[3] N.C. Greenham, X.G. Peng, A.P. Alivisatos, Physical Review B 54 (1996) 17628.
[4] W.U. Huynh, J.J. Dittmer, A.P. Alivisatos, Science 295 (2002) 2425.
[5] V.L. Colvin, M.C. Schlamp, A.P. Alivisatos, Nature 370 (1994) 354.
[6] S. Coe, W.K. Woo, M. Bawendi, V. Bulovic, Nature 420 (2002) 800.
[7] K. Mukai, K. Watanabe, Y. Kimura, Japanese Journal of Applied Physics 49 (2010) 04DH07.
[8] V.K. LaMer, R.H. Dinegar, Journal of the American Chemical Society 72 (1950) 4847.
[9] M.A. Hines, G.D. Scholes, Advanced Materials 15 (2003) 1844.
[10] L. Cademartiri, J. Bertolotti, R. Sapienza, D.S. Wiersma, G. Freymann, G.A. Ozin, Journal of Physical Chemistry B 110 (2006) 671.
[11] H. Zhao, M. Chaker, D. Ma, Journal of Physical Chemistry C 113 (2009) 6497.
[12] H. Zhao, T. Zhang, M. Chaker, D. Ma, Journal of Nanoscience and Nanotechnology 10 (2010) 4897.
[13] S.F. Wang, F. Gu, M.K. Lü, G.J. Zhou, A.Y. Zhang, Journal of Crystal Growth 289 (2006) 621.
[14] B. Ding, M. Shi, F. Chen, R. Zhou, M. Deng, M. Wang, H. Chen, Journal of Crystal Growth 311 (2009) 1533.
[15] C.B. Murray, D.J. Norris, M.G. Bawendi, Journal of the American Chemical Society 115 (1993) 8706.